Sahar Zolfaghari[1], Amin Rabiei Baboukani[1], Ali Ashrafi[2], Ahmad Saatchi[3]*

[1]Islamic Azad University, Advanced Materials Research Center, Materials Engineering Department, Najafabad Branch, Najafabad, Iran, [2]Isfahan University of Technology, Department of Materials Engineering, Isfahan, Iran, [3]University of Wisconsin, Department of Materials Science and Engineering, Madison, USA.

Scientific paper
ISSN 0351-9465, E-ISSN 2466-2585
UDC:620.197.3
doi: 10.5937/ZasMat1801110Z

Zastita Materijala 59 (1)
108 - 116 (2018)

Investigation the effects of Na_2MoO_4 as an inhibitor on electrochemical corrosion behavior of 316L stainless steel in LiBr solution

ABSTRACT

The effect of sodium molybdate (Na_2MoO_4) as an inhibitor at various concentrations of 50, 100 and 200ppm on the electrochemical corrosion behavior of 316L stainless steel in LiBr solution at 60°C was studied by polarization curves, electrochemical impedance spectroscopy (EIS) methods and electron microscopy. Polarization curves indicate that Na_2MoO_4 acts as mixed-type inhibitor. The corrosion resistance of 316L stainless steel samples increases with the inhibitor concentration up to 200ppm. By increasing the inhibitor concentration from 50ppm to 200ppm, corrosion current density decreases. These results were confirmed by further analysis using a scanning electron microscope.

Keywords: *sodium molybdate, corrosion, 316L stainless steel, Lithium bromide.*

1. INTRODUCTION

Corrosion has been one of the most critical fields of study for many years. Researchers have tried different approaches such as applying coatings or using some specific ceramics because of their high chemical stability [1-5].

However, despite the outstanding corrosion resistivity of ceramics, steel is still one of the most applicable materials in industry. Therefore, it is essential to enhance its corrosion resistivity under severe conditions such as high temperatures in heat exchangers [6-11].

Lithium bromide (LiBr) has been widely used in absorption refrigeration systems due to its favorable thermophysical properties. Circulation of LiBr solution within the pumps and pipes are required during the operation of these systems [12-19]. Although LiBr possesses favorable thermophysical properties, it can cause serious corrosion problems in the metallic components in refrigeration systems and heat exchangers in absorption plants [20-23] . Other disadvantages of the LiBr/water mixtures are: a) low working pressure, b) high corrosion rates at high temperatures, and c) tendency to crystallize at high LiBr concentrations. However, there are not data available concerning the corrosion problems caused by LiBr [24, 25].

Generally, stainless steels are not corrosion resistant in aggressive environments and they are prone to local corrosion including pitting corrosion [26, 27]. This form of corrosion is very destructive and dangerous because of the possibility of material perforation. Stainless steels are widely used in absorption systems components such as condensers, evaporators and absorbers due to their high corrosion resistance [28, 29]. Among the different stainless steels, austenitic ones and specially AISI 316L SS are often used for its high corrosion resistance. However, due to factors such as high temperature and LiBr concentration, stainless steels can suffer from severe corrosion problems. For this reason, the expected high corrosion effects of the LiBr aqueous solutions guide us to use corrosion inhibitors added to these environments. However, there exist very few inhibitors, which satisfy both technological and ecological requirements at the same time [30,31]. Normally, inhibitors are used for corrosion control in closed systems. The functionality of some corrosion inhibitors depends on the type of material, its properties and the corrosive environment. Chromate (CrO_4^{2-}) is a very effective passivating inhibitor at relatively high levels. It is

*Corresponding author: Amin Rabiei Baboukani
E-mail: Amin_rab22@yahoo.com
Paper received: 05. 11. 2017.
Paper accepted: 25. 12. 2017.
Paper is available on the website: www.idk.org.rs/journal

very effective for ferrous alloys in the presence of halide ions. It can passivate metals by forming mono-atomic or polyatomic oxide film on the electrode surface. Thus, chromates are very good inhibitors to prevent pitting corrosion for stainless steels. Nitrates (NO_3^{2-}) and molybdates (MoO_4^{2-}) are inorganic, passivating inhibitors, which have been used in many corrosive environments. For instance, molybdates have been used to prevent mild steel and cold rolling steel [32,33] corrosion in simulated cooling water, acidic solutions [34, 35]. They can also be used to seal phosphate coatings on hot-dip galvanized steel [36,37] or on the bacterial corrosion or iron [38,39].

In 1953, Robertson first studied the inhibitive effect of MoO_4^{2-} on the corrosion of carbon steel in neutral solution [40]. Afterwards, there are many papers in the literature concerning the application of MoO_4^{2-} as an effective inhibitor for corrosion of steel in neutral or approximate neutral media [41]. Besides steel, magnesium alloy in simulated cooling water have been protected against corrosion using MoO_4^{2-} [42,43].

However, to the best of our knowledge, there are a few studies on for MoO_4^{2-} as a corrosion inhibitor for 316L SS in LiBr solution. Thus, the goal of this work is to evaluate the corrosion rate of 316L type stainless steel (316L SS) in the LiBr and evaluate the use of $NaMoO_4^{2-}$as less toxic and cheaper inhibitors.

2. EXPERIMENTAL

2.1. Materials

316L type stainless steel with the chemical composition shown in Table 1 was used as an experimental material. The steel was purchased as sheet with dimensions of 1500x1200 x 1.5 mm). The surfaces of the substrates were prepared through grinding via 240, 400, 600, and 800-grade SiC papers, and rinsing with distilled water. In this study, 850gr/l LiBr was a commercial test solution. Potentiodynamic experiments were carried out in 0ppm to 200ppm sodium molybdate as an inhibitor. All tests were conducted at 60°C.

Table 1. Chemical composition of L316 stainless steel

Tabela 1. Hemijski sastav L316 nerđajući čelik

C	Mn	Si	P	S	Cr	Mo	Ni	Fe
0.03	2	0.75	0.045	0.03	16.5	2.3	10.8	Balance

2.2. Corrosion rate measurements

2.2.1. Potentiodynamic polarization studies

The corrosion parameters of samples in different concentration of sodium molybdate were studied using potentiodynamic polarization in LiBr solution. The potentiodynamic polarization experiments were conducted by sweeping the potential at a scan rate of 1 mVs^{-1} in the range of -250mV to +500mV versus open circuit potential (OCP) using PARSTAT 2273 advanced electrochemical system (Princeton Applied Research). The results were analyzed via Tafel extrapolation theory. Tafel plots were obtained from the data and the corrosion current density (Icorr) was determined by extrapolating the straight-line section of the anodic and cathodic Tafel lines. In order to have a better comparison between the results obtained by the electrochemical methods, all measurements were carried out in the same conditions. Hence, for all tests, three-electrode set up including working electrode (test samples), platinum auxiliary electrode, and a saturated calomel reference electrode (SCE) were used for the corrosion studies. Before any electrochemical test, the samples were left to stabilize for 30 min. Pitted surfaces of the working electrode AISI 316Ti after potentiodynamic polarization tests were observed by a scanning electron microscope (SEM), TESCAN-XMU model. After potentiodynamic polarization tests in LiBr solution with and without inhibitor addition, the samples were cleaned ultrasonically in alcohol to remove the corrosion products from surface.

2.2.2. Electrochemical impedance spectroscopy (EIS)

In order to better understand the corrosion behavior of samples in terms of corrosion resistance, the impedance spectra were acquired in the frequency range of 100kHx to 10mHz in LiBr solution. The impedance data was modeled using Zview software.

3. RESULTS AND DISCUSSION

3.1. Corrosion measurements

The open circuit potential is a parameter which indicates the tendency of a material to electrochemical oxidation in a corrosive medium based on thermodynamics. This potential may vary with time due to the changes in the nature of the surface of the electrode (oxidation, formation of the passive layer or immunity). In figire 1, open circuit diagrams, shows potential changes with time for solution in the absence and presence of sodium molybdate in different concentration. According to the figure, in the absence of inhibitor, the trend is

towards the positive potential values [44]. This indicates that the sample in this case is corroded and the corrosion product is formed on it, which in turn has a higher potential. With the addition of 50ppm Na_2MoO_4, the initial value of the potential shifted to the higher values, which caused the formation of the protective layer by the absorption of inhibitor on the surface of sample but the changes of the potential values are not stable and show that complete inhibition does not occur. These changes can also be seen in the presence of 100ppm inhibitor. According to figure 1, sample with 200ppm sodium molybdate is the most stable state. In this sample, although the potential is lower than 50ppm and 100ppm but it suggests that by adsorption, corrosion is prevented at the early stages.

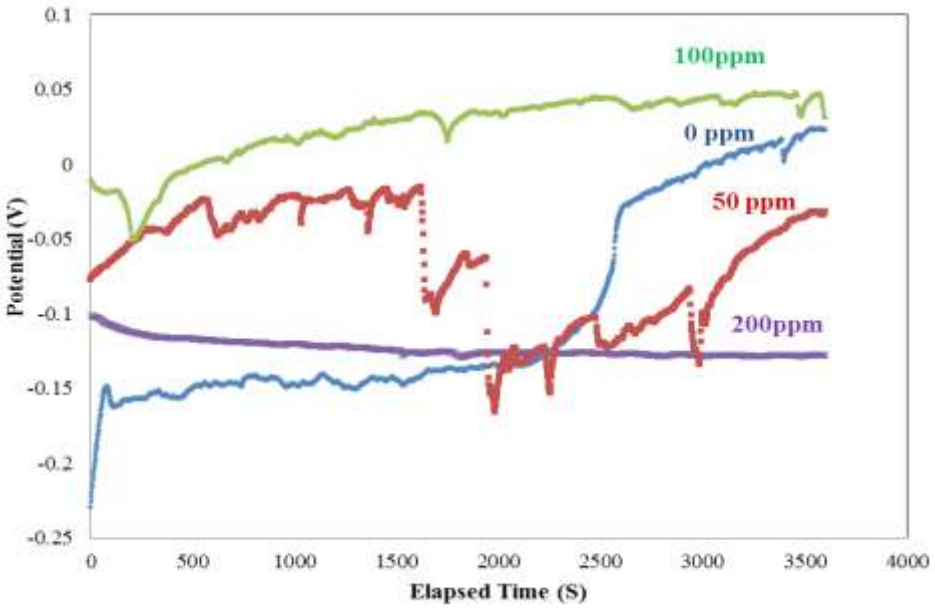

Figure 1. Open circuit potential versus time for the 316L stainless steel samples in LiBr solution with various Na_2MoO_4 concentrations.

Slika 1. Potencijal otvorenog kola u odnosu na vreme za uzorke 316L od nerđajućeg čelika u LiBr rastvoru sa različitim koncentracijama Na_2MoO_4

Figure 2 shows the electrochemical results obtained from the polarization studies for 316L stainless steel samples in LiBr solution containing various concentrations of Na_2MoO_4 at 60°C. The electrochemical corrosion parameters obtained from the polarization curves are summarized in Table 2. According to polarization tests, all three inhibitor concentrations lead to relatively higher corrosion resistivity of samples in the LiBr solution. The presence of the inhibitor shifts the polarization curves to the lower values of current densities [45]. In other words, the stainless steel corrosion is hindered by Na_2MoO_4. According to the results in Table 2, Na_2MoO_4 is considered as absorption inhibitors.

By increasing the concentration of the inhibitor, more anode active sites are covered and also in cathode sites, the hydrogen progression is prevented. In this context, decreasing the corrosion current density is associated with increasing the concentration of inhibitor in the solution and according to Figure 2 and Table 2, the lowest corrosion current density is for 200ppm sodium molybdate. As we can see the higher inhibitor concentration (200ppm) caused the extension of the passive region to higher positive potential values [46]. According to Table 2, the anodic and cathodic slopes have changed and this suggests that sodium molybdate acted as mixed-type inhibitors.

Table 2. Corrosion parameters of stainless steel in LiBr solution at 60°C in the presence of Na_2MoO_4

Tabela 2. Parametri korozije nerđajućeg čelika u LiBr rastvoru na 60°C u prisustvu Na_2MoO_4

Inhibitors Concentration (ppm)	E_{corr} (mv)	I_{corr} (A)	$_c$(mv)β	$_a$(mv)β
0	-194	9×10^{-6}	50	45
50	-192	2×10^{-6}	87	64
100	-101	5×10^{-7}	59	41
200	-120	2×10^{-7}	99	93

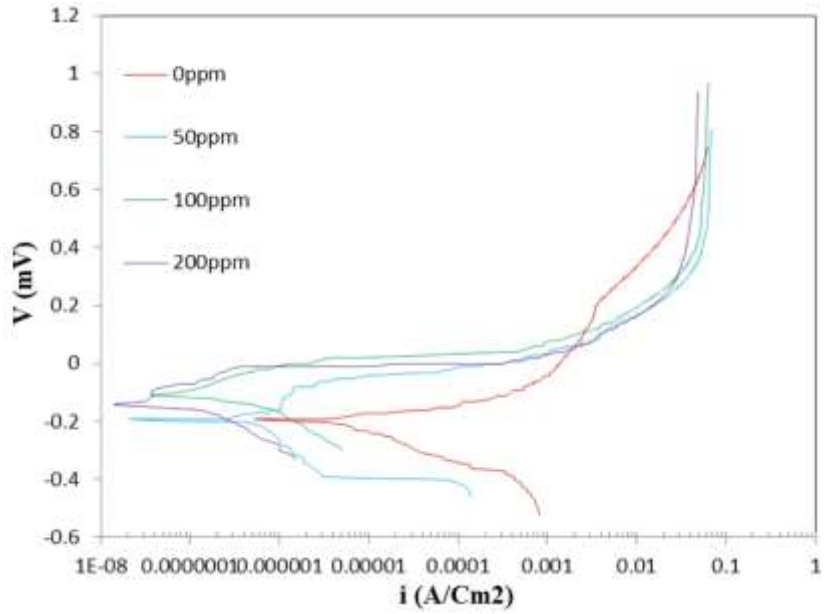

Figure 2. Potentiodynamic polarization curves of type 316L SS obtained in LiBr solution with various Na_2MoO_4 concentrations at 60°C.

Slika 2. Potentiodinamičke krive polarizacije za čelik 316L SS dobijene u LiBr rastvoru sa različitim koncentracijama Na_2MoO_4 na 60°C.

In order to further understand the corrosion behavior, samples were examined by Electrochemical impedance spectroscopy (EIS). Figure 3 represents the Nyquist and Bode's diagrams for 316L SS in LiBr solution without and with various concentrations of Na_2MoO_4 at 60°C. The Nyquist plots for all samples exhibit a semicircle shape and the sizes of the loops are different from each other. As it stands, there is one time constant in the absence of sodium molybdate. This time constant is related to the electrical double layer on the surface of the sample indicating that there is a mechanism for corrosion of the substrate. This mechanism is primarily related to the double layer between the metal and solution [47].

In the presence of inhibitor, based on Bode diagrams, there are two time constants, suggesting that this is the surface film, which controls the corrosion reactions. By increasing the charge transfer resistance for this film and by increasing the inhibitor concentration, better protective and compact film is made. The second time constant values can be charge transfer reactions at the interface of the surface film caused by inhibitor and the surface of 316L stainless steel [48].

A more detailed interpretation of the EIS measurements was performed by fitting the experimental plots using equivalent electrical circuit models which were proposed in order to simulate the electrochemical behavior of the studied coatings. These models were based on the combination of resistances, capacitances, and other elements that should have a physical meaning, related to the electrochemical response of the system [46,49]. In this work, two equivalent electrical circuit models were used, which are presented in Figure 4. Table 3 presents the electrical parameter values found by fitting the equivalent electrical circuit from the experimental EIS data, obtained in a LiBr solution. In these circuits, Rs, Rp and Rinh represent the electrolyte resistance, polarization resistance and resistance at the interface of solution and inhibitor, respectively. According to figure 3, C_{dl} represents double layer capacitance and C_{inh} represents a capacitance at the interface of solution and inhibitor [50,51].

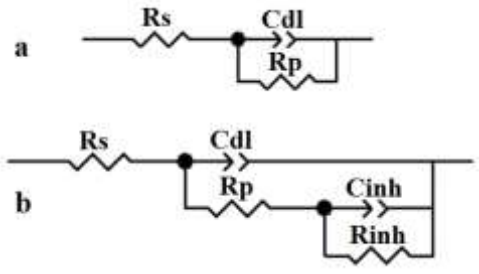

Figure 3. Equivalent circuit for 316L SS samples in LiBr solution, a) absence and b) presence of inhibitor

Slika 3. Ekvivalentno kolo za uzorke čelika 316L SS u LiBr rastvoru, a) odsustvo i b) prisustvo inhibitora.

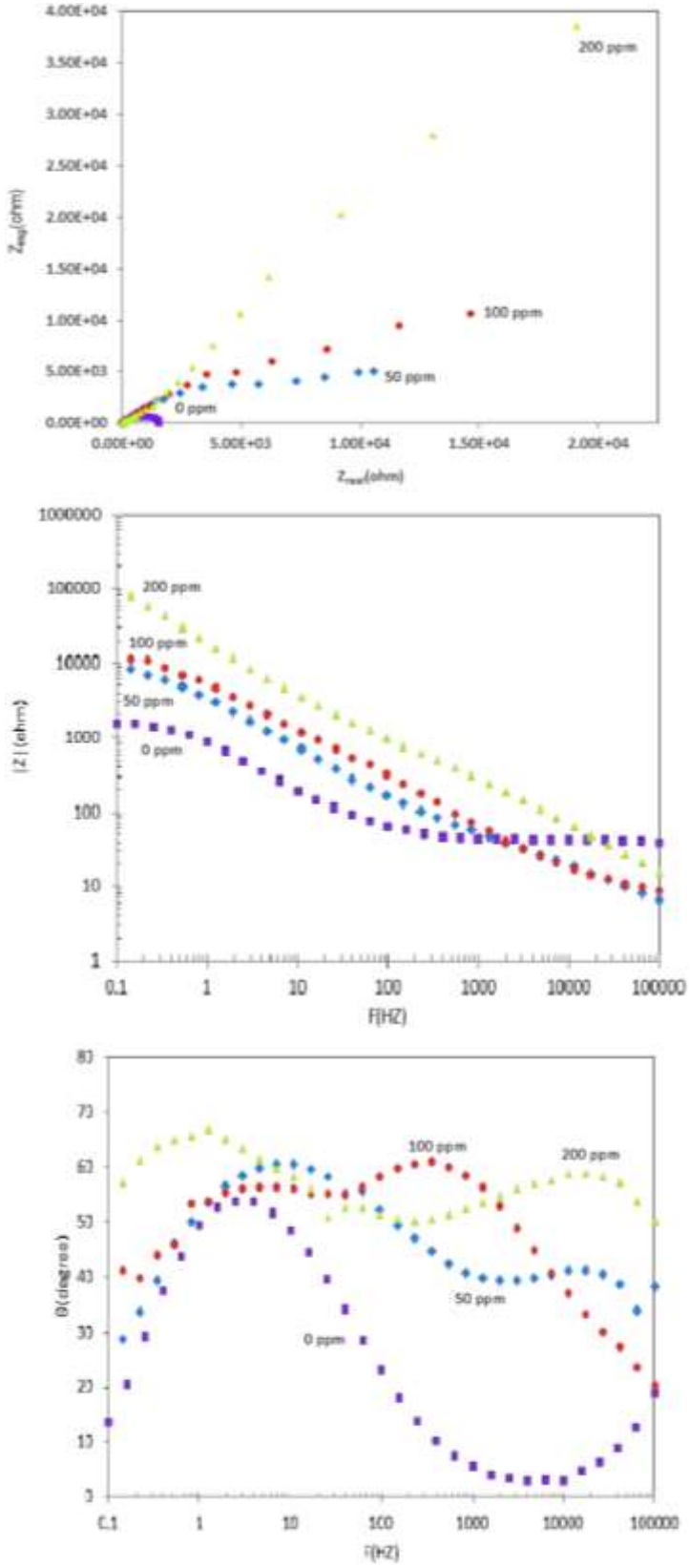

Figure 4. Nyquist and Bode diagrams of type 316L SS obtained in LiBr solution with various sodium molybdate concentrations at 60°C

Slika 4. Nyquist i Bode dijagrami za čelik316L SS dobijeni u rastvoru LiBr sa različitim koncentracijama natrijum molibdata na 60°C

Table 3. EIS parameters for the corrosion of 316L SS in MiBr solution containing different concentrations of Na_2MoO_4 at 60°C

Tabela 3. Parametri EIS za koroziju 316L SS u MiBr rastvoru koji sadrže različite koncentracije Na_2MoO_4 na 60°C

Inhibitor Concentration (ppm)	R_s (Ω)	C_{inh} (F)	R_{inh} (Ω)	Cdl(F)	Rp(Ω)
0	5.155	-	-	2.79×10-4	21000
50	2.54	6.68×10^{-5}	111	1.80×10-5	29800
100	8.218	4.23×10^{-5}	230	8.42×10-6	37322
200	10.04	1.67×10^{-5}	370	3.15×10-7	138000

3.2. SEM investigations

Figure 5 shows the SEM micrographs of 316L stainless steel surface after electrochemical tests in lithium bromide solution containing different concentrations of Na_2MoO_4 at 60°C. In the presence of inhibitor, as expected, the number of pits is decreased in comparison to pure LiBr solution.

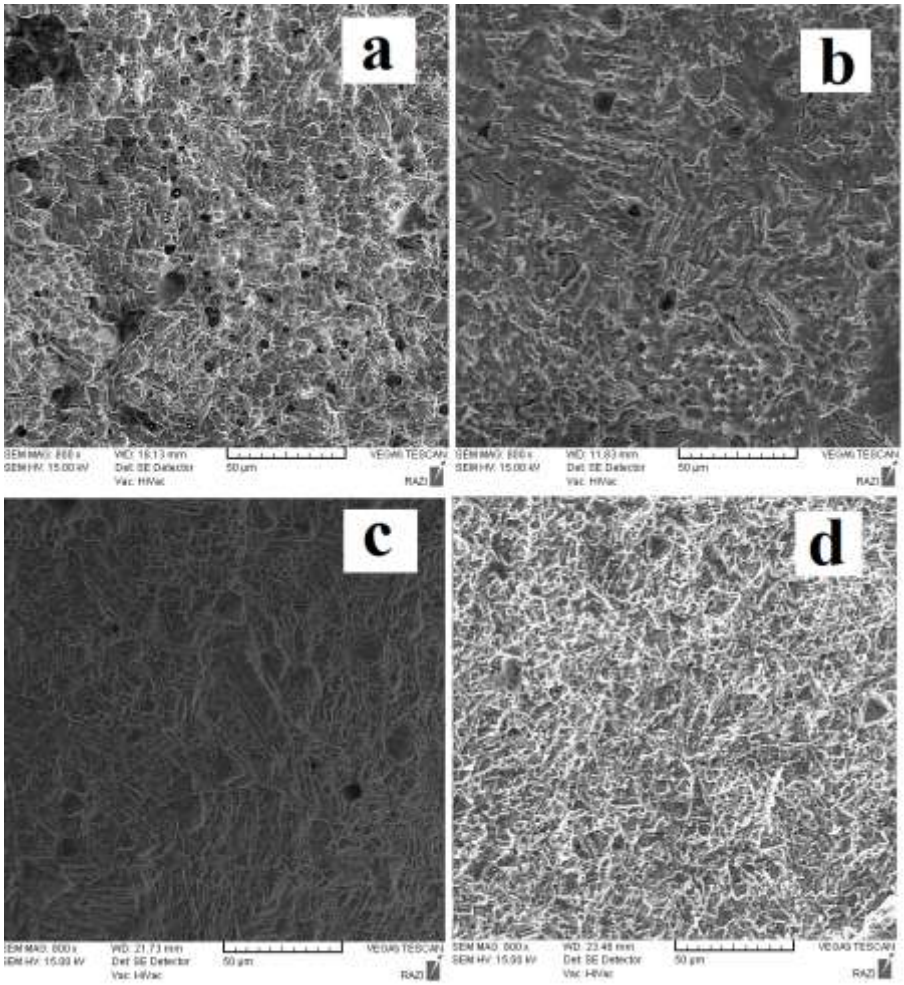

Figure 5. The morphology of pits generated on the surface of 316L SS after the electrochemical test in a) Libr, b) LiBr + 50ppm Na_2MoO_4, c) LiBr + 100ppm Na_2MoO_4 d) LiBr + 200ppm Na_2MoO_4

Slika 5. Morfologija jama nastalih na površini 316L SS posle elektrohemijskog testa u a) Libr, b) LiBr + 50ppm Na_2MoO_4, c) LiBr + 100ppm Na_2MoO_4, d) LiBr + 200ppm Na_2MoO_4

4. CONCLUSION

The corrosion behavior of 316L stainless steel in 850gr/l Lithium bromide in the absence and presence of 50ppm, 100ppm and 200ppm sodium molybdate was studied in this paper. The results could be summarized as below:

1. Potentiodynamic tests revealed that the addition of sodium molybdate to Lithium bromide solution, increases the corrosion resistance of 316L SS. Corrosion resistance increases with the inhibitor concentration.
2. According to the potentiodynamic polarization tests, sodium molybdate was diagnosed as mixed-type inhibitors.
3. Potentiostatic tests revealed that the frequency of pit formation on the surface of 316L stainless steel is decreased in the presence of inhibitor. This result was confirmed by scanning electron microscopy.
4. Impedance test results shows that sodium molybdate is an absorption inhibitor reducing the corrosion rate with its effect on the anodic and cathodic sites simultaneously, the corrosion rate is reduced.

Acknowledgments

The authors are grateful for the technical support of Advanced Materials Research Center, Faculty of Materials Engineering, Najafabad Branch, Islamic Azad University to carry out the above investigations.

5. REFERENCES

[1] G.Shu, J.Che, H.Tian, X.Wang, P.Liu (2017) A compressor-assisted triple-effect H2O-LiBr absorption cooling cycle coupled with a Rankine Cycle driven by high-temperature waste heat, Applied Thermal Engineering(Supplement C), 112, 1626-1637.

[2] A.Rabiei Baboukani, A.Saatchi, R.Ebrahimi-Kahrizsangi (2012) Solid State Displacement Reaction Between Ni and CuO in 1000ºC as a High Temperature Composites, in The 3rd International Conference on Composites: Characterization, Fabrication and Application (CCFA-3).

[3] S.Darvish, Y.Zhong (2017) Quantitative Defect Chemistry Analysis Of (La1-xCax)yFeO3±δ Perovskite, ECS Transactions, 78(1), 565-572.

[4] C.C.Wang, S.He, K.Chen, M.R.Rowles, S.Darvish, Y. Zhong, S. P. Jiang (2017) Effect of SO2 Poisoning on the Electrochemical Activity of La0.6Sr0.4Co0.2Fe0.8O3-δ Cathodes of Solid Oxide Fuel Cells, Journal of The Electrochemical Society, 164(6), F514-F524.

[5] S. Akhavan, A.Rabiei Baboukani, A. Saatchi, R. Ebrahimi-Kahrizsangi, S. Shirmohammadi (2014) Investigating the anodizing process of Aluminum alloys in 0.3M Oxalic acid and its metallurgical and mechanical behavior, in Proceedings of Iran International Aluminum Conference (IIAC2014).

[6] M.Baqersad, A.Hamedi, M.Mohammadafzali, H.Ali (2017) Asphalt mixture segregation detection: Digital image processing approach, Advances in Materials Science and Engineering, 2017, 1-6.

[7] Z.Lu, S.Darvish, J.Hardy, J.Templeton, J. Stevenson, Y. Zhong (2017) SrZrO3 Formation at the Interlayer/Electrolyte Interface during (La1-xSrx)1-δCo1-yFeyO3 Cathode Sintering, Journal of The Electrochemical Society, 164(10), 3097-3103.

[8] P.Foroughi, Z.Cheng (2016) Understanding the morphological variation in the formation of B4C via carbothermal reduction reaction, Ceramics International, 42(14), 15189-15198.

[9] P.Foroughi, Z.Cheng (2015) From micron-sized particles to nanoparticles and nanobelts: structural non-uniformity in the synthesis of boron carbide by carbothermal reduction reaction, Advances in Ceramic Armor XI, Ceramic Engineering and Science Proceedings, 36(4), 51-59.

[10] P.Foroughi, C.Zhang, A.Agarwal, Z.Cheng (2017) Controlling phase separation of TaxHf1−xC solid solution nanopowders during carbothermal reduction synthesis, Journal of the American Ceramic Society, 100(11), 5056-5065.

[11] O.Lopez-Garrity, G.S.Frankel (2017) Corrosion Inhibition of Aluminum Alloy 2024-T3 by Sodium Molybdate., Journal of The Electrochemical Society, 161(3), 95-106.

[12] S.K.Verma, M.S.Mekhjian, G.R.Sandor, N.Nakada (1999) Corrosion inhibition in lithium bromide absorption fluid for advanced and current absorption cycle machines, ASHRAE Transactions, 105, 813-815.

[13] C.Luo, Q.Su (2013) Corrosion of carbon steel in concentrated LiNO3 solution at high temperature, Corrosion Science(Supplement C), 74, 290-296.

[14] M.T. Montañés, R.Sanchez-Tovar, J.García-Antón, V. Perez-Herranz (2010) Influence of the Flowing Conditions on the Galvanic Corrosion of the Copper/AISI 304 Pair in Lithium Bromide Using a ZeroResistance Ammeter, International Journal of Electrochemical Science, 5, 1934-1942.

[15] E.A.Abd El Meguid, N.K.Awad (2009) Electrochemical pitting corrosion behaviour of α-brass in LiBr containing solutions, Corrosion Science, 51(5), 1134-1139.

[16] A.I.Muñoz, J.Garcia Anton, J.L.Guinon, V.Perez Herranz (2004) Corrosion Behavior of Austenitic and Duplex Stainless Steel Weldings in Aqueous Lithium Bromide Solution, CORROSION, 60(10), 982-995.

[17] M.Itagaki, Y.Hirata, K.Watanabe (2003) Anodic dissolution and disproportional reaction of copper in bromide solution investigated by channel flow electrode., Corrosion Science, 45(5), 1023-1036.

[18] E.Sarmiento, J.Uruchurtu, J.G.Gonzalez-Rodriguez, C. Menchaca, O. Sarmiento (2011) Electrochemical Noise Analysis of Type 316L Stainless Steel in a LiBr + Ethylene Glycol + H2O Solution, CORROSION, 67(10), 105004-105012.

[19] A.H.Rezayan, N.Firoozi, S.Kheirjou, S.J. Tabatabaei Rezaei, M.Reza Nahid (2017) Synthesis and Characterization of Biodegradable Semi-Interpenetrating Polymer Networks Based on Star-Shaped Copolymers of ε-Caprolactone and Lactide, Iranian Journal of Pharmaceutical Research : IJPR, 16(1), 63-73.

[20] S.Forouzanfar, N.Talebzadeh, S.Zargari, H.Veladi (2015) The effect of microchannel width on mixing efficiency of microfluidic electroosmotic mixer, in 3rd RSI International Conference on Robotics and Mechatronics (ICROM).

[21] R.Sánchez-Tovar, M.T.Montañés, J. García-Antón (2013) Effects of microplasma arc AISI 316L welds on the corrosion behaviour of pipelines in LiBr cooling systems., Corrosion Science(Supplement C), 73, 365-374.

[22] O.Awadallah, Z.Cheng (2018) Study of the fundamental phase formation mechanism of sol-gel sulfurized Cu2ZnSnS4 thin films using in situ Raman spectroscopy, 176, 222-229.

[23] D.Itzhak, O.Elias (1994) Behavior of Type 304 and Type 316 Austenitic Stainless Steels in 55% Lithium Bromide Heavy Brine Environments, CORROSION, 50(2), 131-137.

[24] Z.Chen, X.Zhang, L.Huang, X.Guo (2012) Atomic force microscopy and electrochemical investigation on the corrosion behavior of carbon steel passivated by molybdate and chromate, Microscopy Research and Technique, 76(2), 173-177.

[25] M.Mafi, H.Azizi, H.Yazdizadeh Alborz (2017) A new model of free global positioning system using Triple DME, International Rsearch Journal of Engineering and Technology (IRJET), 04, 1815-1819.

[26] R.Agrawal, E.Adelowo, A.Rabiei Baboukani, M. Franc Villegas, Al.Henriques, C.Wang (2017) Electrostatic Spray Deposition-Based Manganese Oxide Films—From Pseudocapacitive Charge Storage Materials to Three-Dimensional Microelectrode Integrands, Nanomaterials, 7(8), 198-207.

[27] 27. A.Rabiei baboukani, S.Akhavan, M. Rezvani, E. Ebrahimi-Kahrizsangi, A.Saatchi (2016) Electrochemical Corrosion Behavior of Friction Stir Welded AA6061 in NaCl Solution, in Proceedings of Iran International Aluminum Conference (IIAC2016).

[28] A.Rabiei Baboukani, S.Akhavan, A.Saatchi, R. Ebrahimi-Kahrizsangi, E.Saebnoori (2016) Mechanical Properties of AA2024 In the Presence of Al-Cu Intermetallic Surface Layer, in Proceedings of Iran International Aluminum Conference (IIAC2016).

[29] N.Firoozi, A.Hossein Rezayan, S.J.Tabatabaei Rezaei, M.Mir-Derikvand, M.Nabid, J. Nourmohammadi, J.Mohammadnejad Arough (2017) Synthesis of poly(ε-caprolactone)-based polyurethane semi-interpenetrating polymer networks as scaffolds for skin tissue regeneration, International Journal of Polymeric Materials and Polymeric Biomaterials, 66(16), 805-811.

[30] P.Foroughi, M.Moghadasi (2014) The Effect of Heat Treatment on the Magnetic Properties of Nanocrystalline Fe-Ni-Si Powders, Advanced Materials Research, 829, 693-697.

[31] M.Peiravi, L.Ackah, R.Guru, M.Mohaty, K.Liu, B. Xu, X.Zhu, L.Chen (2017) Chemical extraction of rare earth elements from coal ash., Minerals & Metallurgical Processiing, 34, 170-177.

[32] Z.Cheng, P.Foroughi A.Behrens (2017) Synthesis of nanocrystalline TaC powders via single-step high temperature spray pyrolysis from solution precursors, Ceramics International, 43(3), 3431-3434.

[33] D.Wang, X.Tang, Y.Qiu, F.Gan, G.Z.Chen (2005) A study of the film formation kinetics on zinc in different acidic corrosion inhibitor solutions by quartz crystal microbalance, Corrosion Science, 47(9), 2157-2172.

[34] I.Khakpour, R.Soltani, M.H.Sohi (2015) Microstructure and High Temperature Oxidation Behaviour of Zr-Doped Aluminide Coatings Fabricated on Nickel-based Super Alloy, Procedia Materials Science(Supplement C), 11, 515-521.

[35] R.Rabiei Baboukani, E.Sharifi, S.Akhavan, A. Saatchi (2016) Co Complexes as a Corrosion Inhibitor for 316 L Stainless Steel in H2SO4 Solution, Journal of Materials Science and Chemical Engineering, 4(9), 28-35.

[36] Y.C.Chen, C. M.Lee, S.K.Yen, S.D.Chyou (2007) The effect of denitrifying Fe-oxidizing bacteria TPH-7 on corrosion inhibition of sodium molybdate, Corrosion Science, 49(10), 3917-3925.

[37] K.Moschouris, N.Firoozi, Y.Kang (2016) The application of cell sheet engineering in the vascularization of tissue regeneration, Regenerative Medicine, 11(6), 559-570.

[38] A.M.Cabral, W.Trabelsi, R.Serra, M.F.Montemor, M. L.Zheludkevich, M.G.S.Ferreira (2006) The corrosion resistance of hot dip galvanised steel and AA2024-T3 pre-treated with bis-[triethoxysilylpropyl] tetrasulfide solutions doped with Ce(NO3)3, Corrosion Science, 48(11), 3740-3758.

[39] J. Liu, L. Weinholtz, L. Zheng, M. Peiravi, Y. Wu, D. Chen (2017) Removal of PFOA in groundwater by Fe0 and MnO2 nanoparticles under visible light., Journal of Environmental Science and Health, Part A, 52, 1048-1054.

[40] S. A. M. Refaey, S.S.Abd El-Rehim, F.Taha, M. B. Saleh, R.A.Ahmed (2000) Inhibition of chloride localized corrosion of mild steel by PO43−, CrO42−, MoO42−, and NO2− anions, Applied Surface Science, 158(3), 190-196.

[41] J.Zeng, J.Li, H.Zhu (2014) The Electrochemistry Behaviour of Carbon Steel in 55% LiBr Solution with A-Mo Inhibitor, Advanced Materials Research, 881-883, 1280-1287.

[42] I.A.Kartsonakis, S.G.Stanciu, A. A. Matei, R.Hirstu, A. Karantonis, C. A. Charitidis (2016) A comparative study of corrosion inhibitors on hot-dip galvanized steel, Corrosion Science (Supplement C), 112, 289-307.

[43] H.Hassannejad, M.Moghaddasi, E.Saebnoori, A. Rabiei Baboukani (2017) Microstructure, deposition mechanism and corrosion behavior of nanostructured cerium oxide conversion coating

modified with chitosan on AA2024 aluminum alloy, Journal of Alloys and Compounds (Supplement C), 725, 968-975.

[44] M.Kaseem, J.H.Min, Y.G.Ko (2017) Corrosion behavior of Al-1wt% Mg-0.85wt%Si alloy coated by micro-arc-oxidation using TiO2 and Na2MoO4 additives: Role of current density, Journal of Alloys and Compounds (Supplement C), 723, 448-455.

[45] M.Saugo, D.O.Flamibini, G.Zampieri, S.B.Saidman (2017) Corrosion resistance improvement of nitinol by anodisation in the presence of molybdate ions, Materials Chemistry and Physics (Supplement C), 190, 136-145.

[46] E.Saebnoori, A.Navidinejad, A.Rabiei Baboukani (2016) Mechanism Study and Parameter Optimization of A356 Aluminum Alloy Electrochemical Polishing, in Proceedings of Iran International Aluminum Conference (IIAC2016).

[47] M.Saremi, C.Dehghanian, M.M.Sabet (2006) The effect of molybdate concentration and hydrodynamic effect on mild steel corrosion inhibition in simulated cooling water, Corrosion Science, 48(6), 1404-1412.

[48] A.Chamaani, M.Sara, N.Chawla, B. El.Zahab (2017) Composite Gel Polymer Electrolyte for Improved Cyclability in Lithium–Oxygen Batteries, ACS Applied Materials & Interfaces, 9(39), 33819-33826.

[49] M.Peiravi, S.R.Mote, M.K.Mohanty, J.Liu (2017) Bioelectrochemical Treatment of Acid Mine Drainage (AMD) from an Abandoned Coal Mine Under Aerobic Condition, Journal of Hazardous Materials, 333, 329-338.

[50] M.Safa, A.Chamaai, N.Chawla, B. El-Zahab (2016) Polymeric Ionic Liquid Gel Electrolyte for Room Temperature Lithium Battery Applications. Electrochimica Acta (Supplement C), 213, 587-593.

[51] M.Safa, Y.Hao, A.Chamaani, E.Adelowo, N. Chawla, C.Wang, B.El-zahab (2017) Capacity Fading Mechanism in Lithium-Sulfur Battery using Poly(ionic liquid) Gel Electrolyte, Electrochimica Acta, 258, 1284-1292.

IZVOD

ISPITIVANJE EFEKATA Na_2MoO_4 KAO INHIBITORA NA ELEKTROHEMIJSKO KOROZIONO PONAŠANJE NERĐAJUĆEG ČELIKA 316L U RASTVORU LiBr

Uticaj natrijum-molibdata (Na_2MoO_4) kao inhibitora pri njegovim različitim koncentracijama 50, 100 i 200 ppm na elektrohemijsko korozijsko ponašanje nerđajućeg čelika 316L u LiBr rastvoru na 60°C ispitani su polarizacionim krivinama, metodama elektrohemijske impedansne spektroskopije (EIS) i elektronske mikroskopije. Otpornost na koroziju uzorka nerđajućeg čelika 316L povećava se sa koncentracijom inhibitora do 200ppm. Povećanjem koncentracije inhibitora od 50ppm do 200ppm smanjuje se gustina korozivne struje. Ovi rezultati su potvrđeni daljom analizom koristeći skenirajući elektronski mikroskop.

Ključne reči: *natrijum molibdat, korozija, nerđajući čelik 316L, litijum bromid.*

Naučni rad
Rad primljen: 05. 11. 2017.,
Rad prihvaćen: 25. 12. 2017.
Rad je dostupan na sajtu: www.idk.org.rs/casopis